Overview of radionuclide migration experiments in the HADES Underground Research Facility at Mol (Belgium)

M. AERTSENS[1],*, N. MAES[1], L. VAN RAVESTYN[1] AND S. BRASSINNES[2]

[1] *Expert Group Waste & Disposal, Belgian Nuclear Research Centre, SCK − CEN - Boeretang 200, B-2400 Mol, Belgium, and* [2] *ONDRAF/NIRAS, Kunstlaan 14, B-1210 Brussels, Belgium*

ABSTRACT: *In situ* migration experiments using different radiotracers have been performed in the HADES Underground Research Facility (URF), built at a depth of 225 m in the Boom Clay formation below the SCK−CEN nuclear site at Mol (Belgium). Small-scale experiments, mimicking laboratory experiments, were carried out with strongly retarded tracers (strontium, caesium, europium, americium and technetium). Contrary to europium, americium and technetium which are subjected to colloid mediated transport, the transport of strontium and caesium can be described by the classic diffusion retardation formalism. For these last two tracers, the transport parameters derived from the *in situ* experiments can be compared with the laboratory-derived values. For both tracers, the apparent diffusion coefficients measured in the *in situ* experiments agree well with the laboratory-derived values.

In the large-scale experiments (of the order of metres) performed in the URF, non-retarded or slightly retarded tracers (HTO, iodide and $H^{14}CO_3^-$) were used. The migration behaviour of these tracers was predicted based on models applied in performance assessment calculations (classic diffusion retardation) using migration parameter values measured in laboratory experiments. These blind predictions of large-scale experiments agree well in general with the experimental measurements. Fitting the experimental *in situ* data leads to apparent diffusion coefficients close to those determined by the laboratory experiments. The iodide and $H^{14}CO_3^-$ data were fitted with a simple analytical expression, and the HTO data were additionally fitted numerically with COMSOL multiphysics, leading to about the same optimal values.

KEYWORDS: *in situ* experiments, migration, validation, apparent diffusion coefficient, URL, HADES, Boom Clay, HTO, iodide, $H^{14}CO_3^-$, strontium, caesium, europium, americium, technetium.

The Belgian Nuclear Research Centre (SCK−CEN) and the Belgian Agency for Radioactive Waste and Enriched Fissile Materials (ONDRAF/NIRAS) pioneered studying the geological disposal of high-level nuclear waste in clay formations. Boom Clay has been studied as a potential host formation and is present under the facilities of SCK−CEN in

Mol at a depth between approximately 190 m and 290 m. Due to its very low hydraulic conductivity (around 2.5×10^{-12} m/s; Aertsens *et al.*, 2004; Wemaere *et al.*, 2008), self-sealing properties (Bernier & Bastiaens, 2004; Bastiaens *et al.*, 2007) and a strong sorption capacity for many radionuclides (De Cannière *et al.*, 1996), Boom Clay is envisaged as a potential host formation for nuclear waste disposal in Belgium. The radiological consequences of the release of hazardous radionuclides from the disposed waste are estimated by performance assessment studies (e.g. Marivoet &

© 2013 The Mineralogical Society

Weetjens, 2009) for which the transport parameters in Boom Clay need to be known. These are mainly determined in laboratory experiments using clay cores sampled in the vicinity of the URL. In order to demonstrate that they are also applicable to larger scales of space and time, *in situ* experiments were performed.

In 1980 the construction of the HADES Underground Research Facility (URF) within the Putte Member of the Boom Clay formation (Aertsens *et al.*, 2004) was started. Since then, HADES has been expanded several times (Fig. 1). The facility allows development of appropriate techniques for constructing a repository, waste emplacement (and possible retrieval), construction of engineered barriers, as well as *in situ* investigations of the disposal environment (geochemistry, hydromechanics, radionuclide behaviour, etc.). *In situ* experiments have the advantage that they represent the disposal conditions as closely as possible. They can be used to confirm behaviour on a large scale and over long durations (Wersin *et al.*, 2008) using laboratory experiments (Aertsens *et al.*, 2008a) as demonstrations.

This paper provides an overview of the *in situ* migration experiments performed at HADES, starting by describing the different types of experiments and the corresponding models, followed by the presentation of the modeling results. The transport parameters values derived by laboratory experiments are compared to those obtained from the *in situ* experiments.

TYPES OF EXPERIMENTS

Two types of experiments were performed. The first type concerns retarded tracers. The experiments were performed on the same small scale as laboratory experiments (of the order of centimetres). This type of experiment is merely used for a long-term demonstration. In Fig. 2, a scheme for the experimental set-up is given. An aliquot of strongly retarded tracer, homogenously distributed by spiking on a filter paper or directly on the clay surface, was sandwiched between two back-to-back clay cores. The clay cores were confined in an open-ended diffusion cell mounted on a hollow cylindrical tube (piezometer) installed within the clay surrounding HADES. The open end of the diffusion cell was equipped with a small tube enabling water sampling. This allows collection of the water seeping out of the clay for a radiological assay. After retrieval from the borehole (by overcoring), the tracer profile in the clay cores was determined. This type of experiment is similar to a laboratory percolation experiment (Aertsens *et al.*, 2008a) but, in the *in situ* version, advection is not provided by an externally applied pressure but is caused by the pressure difference between the water pressure at the depth of the URF and the atmospheric pressure (being the pressure in the tunnel of the URF). The tracers used in these experiments were europium, strontium, caesium, americium and technetium. The measurement error (and, consequently, also the error in the mass balance) is below 10%.

The second type of experiment concerns non-retarded or slightly retarded tracers and was conducted on a large scale (of the order of metres). This type of experiment was also used for testing blind predictions. It consists of one or more multi filter piezometers installed in HADES. After drilling a borehole, the piezometer was inserted. Nitrogen gas was flushed through the
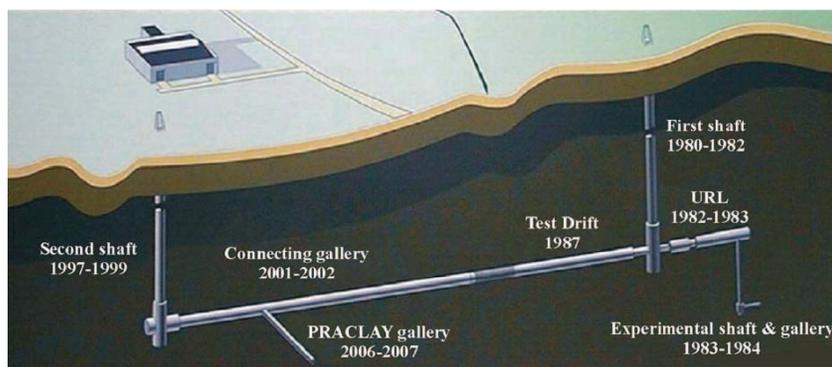

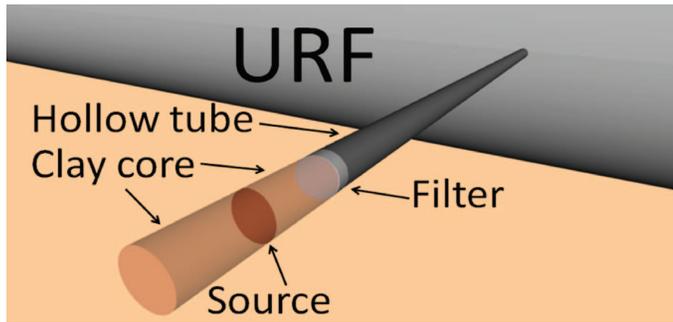Fig. 1. Construction history of the HADES Underground Research Facility.

FIG. 2. Schematic set-up of the small-scale *in situ* experiments for retarded tracers. The hollow tube surrounds both clay cores, preventing tracer migration into the clay surrounding the URF. Both clay cores have a typical length around 3−4 cm and a diameter of 3.8 cm.

filters to prevent oxidation of the clay. Due to the plastic behaviour of the clay, convergence is fast and, after several days, the remaining gap between the piezometer and the borehole wall was completely sealed, preventing the existence of fast transport paths due to voids along the piezometer.

The filters allow water exchange with the Boom Clay and are connected by feeding lines to and from the URF. These feeding lines allow initial injection of tracer into a central filter, as well as permitting regular sampling of the pore water in all filters and measurement of its tracer concentration. The average time between consecutive samplings is a compromise between having enough measurements and avoiding the fact that the filters act as a sink for the water flow around the URF.

Three different experimental set-ups are used. In the CP1 experiment (Put *et al.*, 1993), HTO is injected in the central filter of a horizontal piezometer (Fig. 3). The distance between the centres of consecutive filters is one metre. The Tribicarb-3D experiment (tracers HTO and $H^{14}CO_3^-$) involves three piezometers, of which two are horizontal and one is inclined (Fig. 4 and Table 1). Each piezometer comprises four to eight filters. The TD41HV set-up consists of a vertical and a horizontal piezometer (Fig. 5), each comprising nine filters. This set-up was used in two consecutive experiments: the first with iodide, the second with ^{14}C labelled Natural Organic Matter. Due to the limited half life of $^{125}I^-$ (60 days), the source concentration after three years is below detection limit. Consequently, the experiment was stopped after that time. The remaining experiments are still on-going (some for more than 20 years).

Measurement errors are typically around 15% at low tracer concentrations, decreasing to 5% at
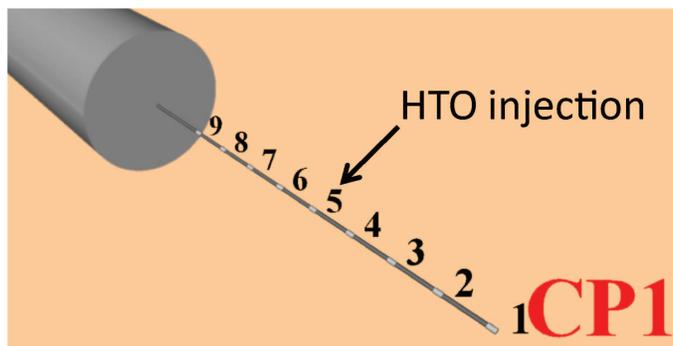

FIG. 3. Set-up of the CP1 experiment: a piezometer with nine filters is placed horizontally next to the URF in Boom Clay. The numbers indicate the filters. The distance between the centres of consecutive filters is one metre. Initially, tracer (HTO) was injected in filter 5.
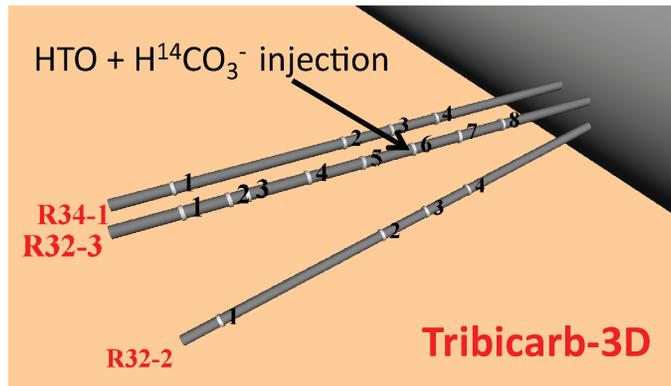
FIG. 4. Set-up of the Tribicarb-3D experiment: three piezometers, each with a number of filters, are placed in the Boom Clay next to the URF. Table 1 contains the filter positions. Both piezometers R34-1 and R32-3 are approximately parallel to one another and to the bedding plane of the clay. Piezometer R32-2 is inclined. Tracer (HTO and $H^{14}CO_3^-$) is initially injected in filter 6 of piezometer R32-3.

higher concentrations. In clay water, $H^{14}CO_3^-$ is unstable and tends to escape the clay water after transforming to the gaseous form of $^{14}CO_2$. In order to prevent the loss of $^{14}CO_2$ due to evaporation (which leads to erroneous measurements), the $H^{14}CO_3^-$ solution injected in Tribicarb-3D as well as the sampled solution were stabilized with sodium hydroxide (NaOH). In the Tribicarb-3D experiment, the activity of both isotopes HTO and $H^{14}CO_3^-$ is determined by liquid scintillation counting. The activity spectra of both isotopes overlap, causing problems when the activity of one isotope dominates the other. Initially, $H^{14}CO_3^-$ concentrations are low (lower than 1000 Bq/l) and the HTO activity is one to two orders of magnitude higher, due to which the $H^{14}CO_3^-$ activity measurements cannot be considered as very reliable.

MODELLING

Transport of a decaying tracer in porous media is described by solutions of the dispersion/advection

TABLE 1. Filter positions in the Tribicarb-3D experiment. Filters where the measured and predicted concentrations are still too low to be measured are not considered.

|	x (m)	Y (m)	Z (m)	Distance to origin (m)	Distance to URF (m)
R32-3 source piezometer					
R32-3-8	−1.985	−0.245	−0.024	2.00	3.00
R32-3-7	−0.992	−0.122	−0.012	1.00	4.00
R32-3-6	**0.000**	**0.000**	**0.000**	**0.00**	5.00
R32-3-5	0.992	0.122	0.012	1.00	6.00
R32-3-4	1.985	0.245	0.024	2.00	7.00
R32-2 inclined piezometer					
R32-2-4	−1.192	0.014	−1.220	1.71	4.00
R32-2-3	−0.219	0.144	−1.410	1.43	5.00
R32-2-2	0.755	0.274	−1.599	1.79	6.00
R34-1 parallel piezometer					
R34-1-4	−0.882	−1.009	−0.042	1.34	4.00
R34-1-3	0.111	−0.889	−0.044	0.90	5.00
R34-1-2	1.103	−0.769	−0.046	1.35	6.00
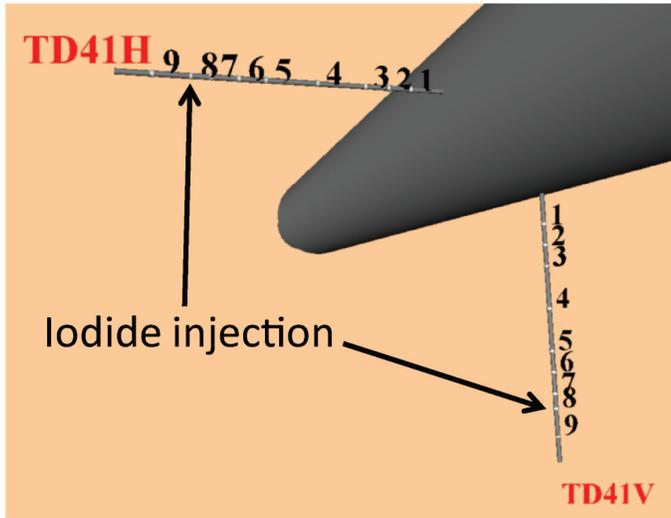
Fig. 5. Set-up of the TD41HV experiment: two piezometers, each with a number of filters, are put in the Boom Clay surrounding the URF. The distance between the centre of the injection filters (filter 8, in both the vertical piezometer TD41V and in the horizontal piezometer TD41H) and the neighboring filter 7, the only one where pore water is sampled, is 0.35 m.

equation (Crank, 1975) complemented with a decay term:

$$\frac{\partial C}{\partial t} = D^i_{app} \frac{\partial^2 C}{\partial x^2} - V_{app} \frac{\partial C}{\partial x} - \lambda C \quad (1)$$

with $C(x,t)$ the tracer concentration in the pore water (Bq/m^3), t time (s), D^i_{app} the apparent dispersion coefficient (m^2/s), x position (m), V_{app} the apparent tracer velocity (m/s) and λ the decay constant (1/s). Recent reviews of transport in clays are in (Bourg, 2004; Altmann *et al.*, 2012).

Modelling the small-scale in situ percolation experiments (retarded tracers)

All tracer is initially in the source (at $x = 0$) which is approximated to be infinitely thin. If zero or only a minor fraction of the tracer has reached the inlet/outlet of a clay core, the tracer distribution $C(x,t)$ in the clay pore water is given by the standard expression (Crank, 1975)

$$C(x,t) = \frac{Q_0}{S\eta R} C_1(x,t,D^i_{app},V_{app}) \exp(-\lambda t) \quad (2)$$

with Q_0 the injected tracer quantity (Bq), S the cross section of the clay cores (m^2), η the diffusion

accessible porosity (dimensionless), R the retardation factor R (dimensionless), and

$$C_1(x,t,D^i_{app},V_{app}) =$$
$$\frac{1}{2\sqrt{\pi D^i_{app}t}} \exp\left(-\frac{(x-V_{app}t)^2}{4D^i_{app}t}\right) \quad (3)$$

The product ηR of the diffusion accessible porosity η (dimensionless) and the retardation factor R (dimensionless) is the ratio V_{Darcy}/V_{app} of the Darcy velocity V_{Darcy} (m/s) and the apparent velocity V_{app}. Because the apparent velocity is determined by the shift of the peak position of the tracer profile (equation 3), which is nearly zero for strongly retarded tracers, the error in the fitted value is large. This type of experiment only leads to accurate values for the apparent dispersion coefficient D^i_{app}. *The apparent velocity V_{app} is sufficiently low to approximate the apparent diffusion coefficient D_{app} (m^2/s) by the apparent dispersion coefficient ($D_{app} = D^i_{app} - \alpha V_{app} \approx D^i_{app}$ with α the dispersion length (m)).* The tracer profile in the clay is the bulk concentration $\eta R\, C(x,t)$.

Introducing the notation L_0 for the distance between the source and the outlet side of the clay core, the tracer quantity $Q_{out}(t)$ (Bq) (the decay is recalculated to zero time) percolated out of the clay

core can be estimated as the amount of tracer stored in a semi-infinite clay core at positions larger than L_0:

$$Q_{out}(t) = \eta R S \int_{L_0}^{\infty} C(y,t)\exp(\lambda t)dy \quad (4)$$

Substituting equations 2, 3 in equation 4 leads to

$$Q_{out}(t) = \frac{Q_0}{2}erfc\left[\frac{L_0 - V_{app}t}{2\sqrt{D_{app}^i t}}\right] \quad (5)$$

In this way, neither the amount of tracer in the filter, nor the tracer in the thin tube connecting the filter to the URF (see Fig. 2), are taken into account. Because the filter and the clay cores are inside the diffusion cell at the end of the piezometer (contrary to the large-scale experiments) there is no water and tracer exchange with the clay surrounding the URF.

Modelling the large-scale in situ percolation experiments: the MICOF model

The injection filter is approximated as a bar shaped source with dimensions $2a$, $2b$ and $2c$. The origin $x = y = z = 0$ is chosen in the middle of this volume and the x axis is parallel to the apparent velocity. The initial condition is

$C(|x| > a, |y| > b, |z| > c, t = 0) = 0$
$C(|x| < a, |y| < b, |z| < c, t = 0) = Q_0/(\eta R 8abc)$ (6)

Solving the three dimensional version of the dispersion/advection/decay equation 1 leads to the tracer concentration

$$C(x,y,z,t) = \frac{1}{8}\frac{Q_0}{\eta R 8abc}\exp(-\lambda t)$$
$$\left(erf\left(\frac{x - V_{app}t + a}{2\sqrt{D_{app,x}^i t}}\right) + erf\left(\frac{a - x + V_{app}t}{2\sqrt{D_{app,x}^i t}}\right)\right)$$
$$\left(erf\left(\frac{y + b}{2\sqrt{D_{app,y}^i t}}\right) + erf\left(\frac{b - y}{2\sqrt{D_{app,y}^i t}}\right)\right)$$
$$\left(erf\left(\frac{z + c}{2\sqrt{D_{app,z}^i t}}\right) + erf\left(\frac{c - z}{2\sqrt{D_{app,z}^i t}}\right)\right) \quad (7)$$

with $D_{app,x}^i$, $D_{app,y}^i$, $D_{app,z}^i$ the apparent dispersion coefficient in the x, y and z directions. If the thickness $2a$ becomes very small, or at sufficiently long times, then $|y_0| \gg a_0$

$$erf\left(\frac{x - V_{app}t + a}{2\sqrt{D_{app,x}^i t}}\right) + erf\left(\frac{a - x + V_{app}t}{2\sqrt{D_{app,x}^i t}}\right) =$$
$$\frac{2}{\sqrt{\pi}}\int_{y_0 - a_0}^{y_0 + a_0}\exp(-y^2)dy \approx$$
$$\frac{2a}{\sqrt{\pi D_{app,x}^i t}}\exp\left(-\frac{(x - V_{app}t)^2}{4\sqrt{D_{app,x}^i t}}\right) \quad (8)$$

with

$$y_0 = \frac{x - V_{app}t}{2\sqrt{D_{app}^i t}} \qquad a_0 = \frac{a}{2\sqrt{D_{app}^i t}} \quad (9)$$

Similar rearrangements for the other directions lead to the point source approximation for the concentration (7):

$$C(x,y,z,t) \approx (Q_0/\eta R)C_1(x,t,D_{app,x}^i,V_{app})$$
$$C_1(y,t,D_{app,y}^i,0)C_1(z,t,D_{app,z}^i,0)\exp(-\lambda t) \quad (10)$$

with C_1 given by equation 3. Comparing equations 10 and 2 shows that basically the large-scale percolation experiments can be considered as a three dimensional version of the small-scale experiments.

In the large-scale experiments, the filter dimensions (e.g. in CP1 the filter length is 8.5 cm and the diameter 4.6 cm) are much smaller than the distance between two consecutive filters (in CP1, one metre), justifying the point source approximation in all filters except the source filter. In the source filter, the filter dimensions are numerically only significant for small times (similar to the small-scale model, where the source is sufficiently small to omit its width). For the filter dimensions the approximation $a = b = c$ is used. The remaining value $a = b = c$ is calculated by putting the bar volume $8abc = 8a^3$ equal to the water volume inside a filter.

MICOF assumes that all around the URF the apparent velocity $\overrightarrow{V_{app}}$ is the same. This is not correct; the water flow around the URF (and therefore also the apparent velocity) is directed towards the centre of the gallery and is not parallel at all sites in the clay. Similarly, due to mass

conservation of water flow towards a cylindrical gallery, the Darcy velocity (and thus the apparent velocity) depends on the distance from the centre of the gallery; its value is not constant, as supposed in MICOF. Although not correct, the approximations just mentioned hardly influence the MICOF predictions as advection in Boom Clay is weak and transport is dominated by diffusion (Henrion *et al.*, 1985). By applying a more sophisticated and more complex model for the large-scale experiments, where the mathematics of the model are solved numerically by the COMSOL code (Weetjens *et al.*, 2011; Weetjens & Maes, 2013), these assumptions are avoided, but it leads numerically to nearly the same predictions as with MICOF.

The MICOF model (equation 7) has five transport parameters: the apparent dispersion coefficients $D^i_{app,x}$, $D^i_{app,y}$, $D^i_{app,z}$, the capacity factor ηR and the apparent velocity V_{app}. The three apparent dispersion coefficients are assumed to be equal to the corresponding diffusion coefficients. Due to the layered structure of the clay, two of these diffusion coefficients are equal and two values remain: the apparent diffusion coefficient parallel to the bedding plane $D_{app,//}$ and the apparent diffusion coefficient perpendicular to the bedding plane $D_{app,\perp}$. The apparent velocity V_{app} is the ratio $V_{Darcy}/\eta R$, and the Darcy velocity V_{Darcy} is the product of the hydraulic conductivity and the pressure gradient around the URF (e.g. Aertsens *et al.*, 2008b). For CP1 a value $V_{Darcy} = 6 \times 10^{-11}$ m/s is used; for Tribicarb-3D and TD41HV, V_{Darcy} is 7.6×10^{-11} m/s. Fitting the experiment, only the diffusion coefficients $D_{app,//}$ and $D_{app,\perp}$ are varied. Due to the simple set-up of the experiment, the modelling is relatively simple (Yi *et al.*, 2012; Naves *et al.*, 2012; Samper *et al.*, 2010).

THE SMALL-SCALE *IN SITU* PERCOLATION EXPERIMENTS

Experiments are carried out with strontium, caesium, europium, americium and technetium. Because europium, americium and technetium transport in Boom Clay is affected by the interaction with organic colloids (Maes *et al.*, 2011), the classic diffusion retardation formulation cannot be used to model successfully the corresponding tracer profiles (Put *et al.*, 1989; Noynaert, 2000; Baston *et al.*, 2002).

Fitting the strontium tracer profile (duration of the experiment 260 days, Fig. 6) leads to an accurate value for the apparent dispersion coefficient: $D^i_{app} = 7 \times 10^{-12}$ m²/s (Aertsens *et al.*, 2009). The percolated amount of strontium (≈ 5 cps) is much smaller than predicted by the model (≈ 240 cps), using the parameter values fitted from the profile. As in Opalinus Clay (Wersin *et al.*, 2008), the *in situ* measured value for the apparent dispersion coefficient is about the same as the values measured in laboratory experiments, which are: 9×10^{-12} m²/s, 6×10^{-12} m²/s, 8×10^{-12} m²/s, 7×10^{-12} m²/s and 6×10^{-12} m²/s (Aertsens *et al.*, 2009a).

Similar to strontium, a clear profile (after a duration of 6.93 years) was observed for caesium (Fig. 7). No tracer leached out of the clay core. The profile leads to an apparent dispersion coefficient $D^i_{app} = 1.0 \times 10^{-13}$ m²/s (and $\eta R \approx 1100$). The value of the apparent dispersion coefficient is similar to the values measured in two laboratory percolation experiments (1.9×10^{-13} m²/s and 1.6×10^{-13} m²/s; Maes *et al.*, 2008) and an electromigration experiment (1.2×10^{-13} m²/s; Maes *et al.*, 2008).
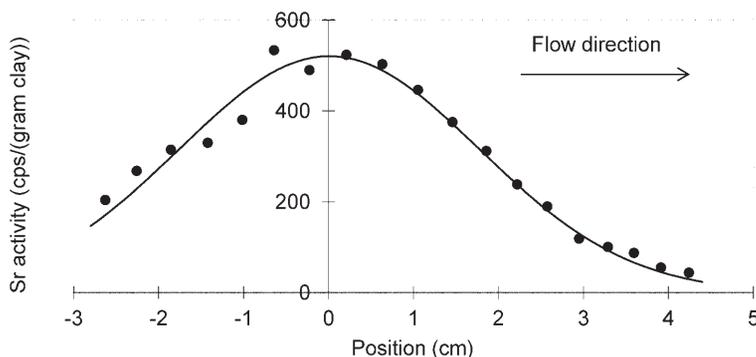

FIG. 6. Strontium profile measured in the clay cores after about 260 days.
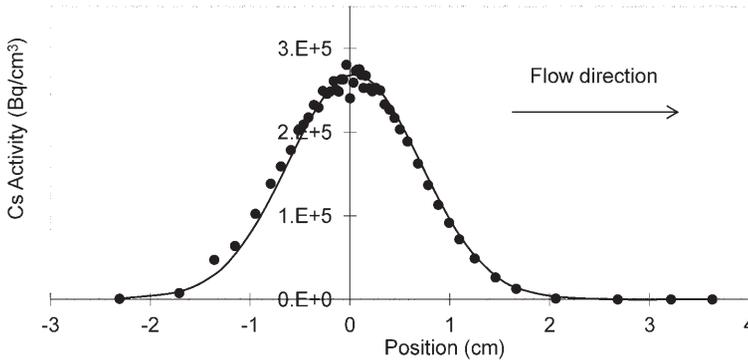
Fig. 7. Caesium profile measured in the clay cores after about 7 years.

THE LARGE-SCALE *IN SITU* PERCOLATION EXPERIMENTS

Except for the ^{14}C labelled Natural Organic Matter injection in TD41HV, blind predictions were made for each experiment. Table 2 lists the transport parameter values used for the blind predictions, the values determined from laboratory experiments and the values obtained by fitting. Since the start of the *in situ* experiments, new laboratory experiments were performed, resulting in laboratory values for $D_{app,//}$, and $D_{app,\perp}$ and ηR which can differ slightly from the values used at the time the blind predictions (see Table 2) were done. Table 2 lists for each experiment the $D_{app,//}$ and $D_{app,\perp}$ values fitted with the ηR value used for the blind prediction as well as the $D_{app,//}$ and $D_{app,\perp}$ values fitted with the most recent ηR value. Both HTO and iodide are considered as unretarded. $H^{14}CO_3^-$ is

TABLE 2. Summary of the transport parameters for the large-scale *in situ* tests at HADES. Comparison of the values determined in the laboratory, the values used for the blind MICOF prediction and the values that were fitted with MICOF or COMSOL. The laboratory values are taken from: $D_{app,//}$ (HTO): average of the values in (Aertsens *et al.*, 2009b, Fig. 2) and the values in (Moors, 2005, table 6.3.3.1); $D_{app,\perp}$ (HTO and iodide) from Aertsens *et al.*, 1999; $D_{app,//}$ ($H^{14}CO_3^-$): average of the values in (Aertsens *et al.*, 2009b, Fig. 2); $D_{app,\perp}$ ($H^{14}CO_3^-$) from Aertsens *et al.*, 2008b; $D_{app,//}$ (iodide) from Bruggeman *et al.*, 2010.

|		Source	$D_{app,//}$ (m²/s)	$D_{app,\perp}$ (m²/s)	ηR
Laboratory	HTO		4.1×10^{-10}	2.3×10^{-10}	0.37
CP1	HTO	MICOF blind prediction	4.0×10^{-10}	2.0×10^{-10}	0.35
		MICOF fit	4.2×10^{-10}	3.1×10^{-10}	0.35
		MICOF fit	4.2×10^{-10}	2.8×10^{-10}	0.37
		COMSOL fit	4.2×10^{-10}	2.4×10^{-10}	0.37
Tribicarb-3D	HTO	MICOF blind prediction	4.1×10^{-10}	2.0×10^{-10}	0.35
		MICOF fit	5.0×10^{-10}	2.0×10^{-10}	0.35
		MICOF fit	5.0×10^{-10}	2.0×10^{-10}	0.37
		COMSOL fit	5.1×10^{-10}	2.1×10^{-10}	0.37
Laboratory	$H^{14}CO_3^-$		1.1×10^{-10}	6.0×10^{-11}	0.26
Tribicarb-3D	$H^{14}CO_3^-$	MICOF blind prediction	1.2×10^{-10}	5.8×10^{-11}	0.33
		MICOF fit	1.0×10^{-10}	7.0×10^{-11}	0.33
		MICOF fit	1.0×10^{-10}	1.1×10^{-10}	0.26
Laboratory	Iodide		3.4×10^{-10}	1.4×10^{-10}	0.16
TD41HV	Iodide	MICOF blind prediction	2.7×10^{-10}	1.4×10^{-10}	0.15
	Iodide	MICOF fit	2.6×10^{-10}	1.5×10^{-10}	0.15
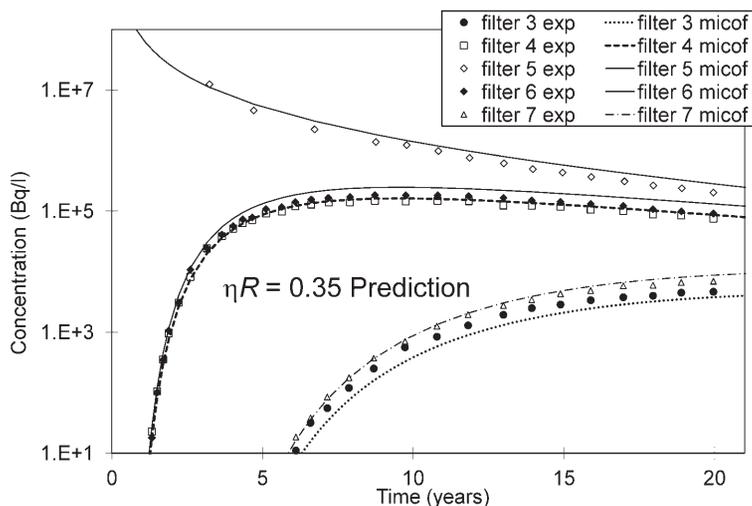
FIG. 8. Blind prediction with the MICOF model and experimental data of the CP1 experiment in five filters.

retarded at high ionic strengths (Aertsens *et al.*, 2009b) and possibly slightly retarded under Boom Clay conditions (Aertsens *et al.*, 2008b).

HTO migration in CP1 and Tribicarb-3D

For CP1, the scatter in the experimental data is small and the agreement with the blind prediction is very good (Fig. 8). As the CP1 piezometer is placed horizontally (Fig. 3), it is evident that the diffusion coefficient parallel to the bedding plane $D_{app,//}$ is the dominant fit parameter. This follows from the

very small fit error (<1%), but also from Table 2, showing that all fits lead to the same $D_{app,//}$ value, while the difference between the optimal $D_{app,\perp}$ values is larger. Despite its simplicity and its crude approximations, the MICOF model leads to the same optimal $D_{app,//}$ value as the more sophisticated COMSOL code, as well as to a similar $D_{app,\perp}$ value. Clearly, the agreement between the $D_{app,//}$ and $D_{app,\perp}$ values determined in the laboratory and the fitted ones from the CP1 experiment is very good. The fitted data coincide very well with the experimental results (Fig. 9). For a comparison of
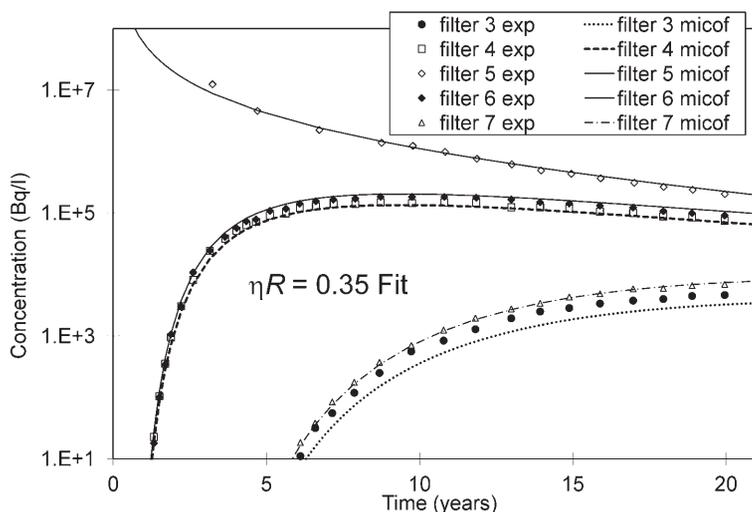

FIG. 9. Experimental data and MICOF fit result of the CP1 experiment.

the MICOF and COMSOL results, both codes use the same V_{app} and ηR values.

The scatter in the Tribicarb-3D HTO data is higher than for CP1, but still limited (Fig. 10). The disagreement between the MICOF prediction and the experimental data is larger than in CP1, but still acceptable. In general, the prediction is similar to, or lower than the experimentally measured concentration. Fitting leads to the same optimal parameters for the MICOF model as for the COMSOL code.
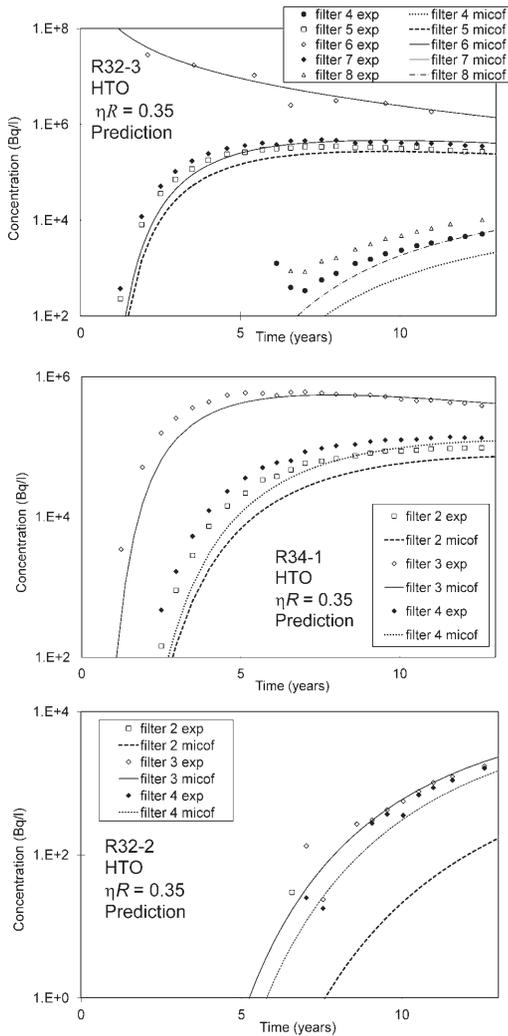
The optimal $D_{app,\perp}$ value agrees very well with the value determined in the laboratory. The value for $D_{app,//}$ is about 25% higher than the laboratory value, which is almost identical to the CP1 optimal $D_{app,//}$ value. The agreement between the fitted and experimental data is very good (Fig. 11).

$H^{14}CO_3^-$ migration in Tribicarb-3D

The large scatter at low concentrations (Fig. 12) is consistent with the explanation already given that this tracer is difficult to measure accurately in that case. Thus, it is not surprising that the disagreement
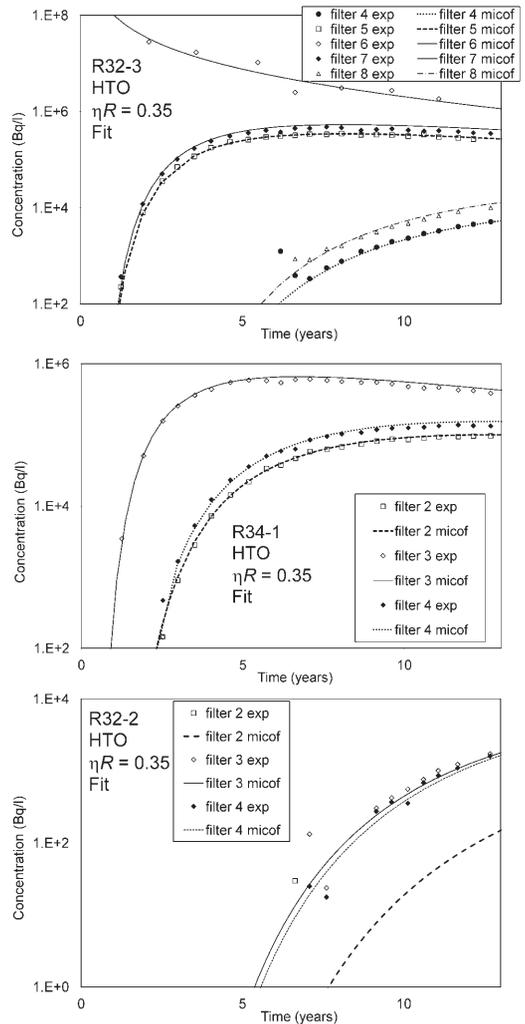

FIG. 10. Blind prediction and experimental data in filters of the injection piezometer R32-3, the piezometer R34-1 parallel to the injection piezometer, and the inclined piezometer R32-2 of the Tribicarb-3D experiment (tracer: HTO).

FIG. 11. Experimental data and fit in the filters of the Tribicarb-3D experiment (tracer: HTO).

between the experimental data and the MICOF prediction is large. After longer times, for the piezometers R32-3 and R34-1 the agreement between the prediction and experimental data is better.

The ηR value used for the blind prediction (ηR = 0.33) differs considerably from the most recently determined laboratory value (ηR = 0.26) (Table 2).
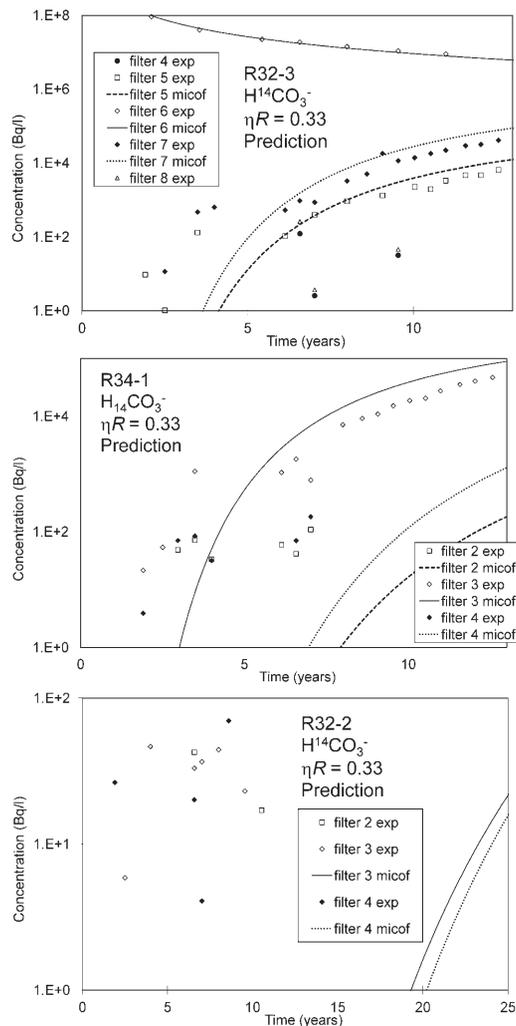
Fitting with ηR = 0.33 leads to the same optimal $D_{app,//}$ value (Table 2) as fitting with ηR = 0.26. The optimal $D_{app,//}$ value is about the same as the lab value. The optimal $D_{app,\perp}$ is ~50% higher for ηR = 0.26 than for ηR = 0.33, where the optimal value is close to the laboratory value. At ηR = 0.26, the optimal $D_{app,//}$ and $D_{app,\perp}$ are about equal, which, considering the anisotropy of the clay, is not realistic. Both fits (ηR = 0.33 and ηR = 0.26) lead to about the same predicted concentrations, which agree well with the experimental data (Fig. 13).

Iodide migration in TD41HV

Iodide was injected simultaneously into the central filters of both the vertical and horizontal piezometers. For both injections, the tracer concentration was only measured in the nearest neighbouring filter. The predicted tracer concentration in the source filter is systematically significantly lower than the measured data (Fig. 14). In the nearest neighbouring filter, the

FIG. 12. Blind prediction and experimental data in the filters of the injection piezometer R32-3, the piezometer R34-1 parallel to the injection piezometer, and the inclined piezometer R32-2 of the Tribicarb-3D experiment (tracer: $H^{14}CO_3^-$). In the filters for which no MICOF prediction is shown, the prediction is lower than the lowest value in the figure.
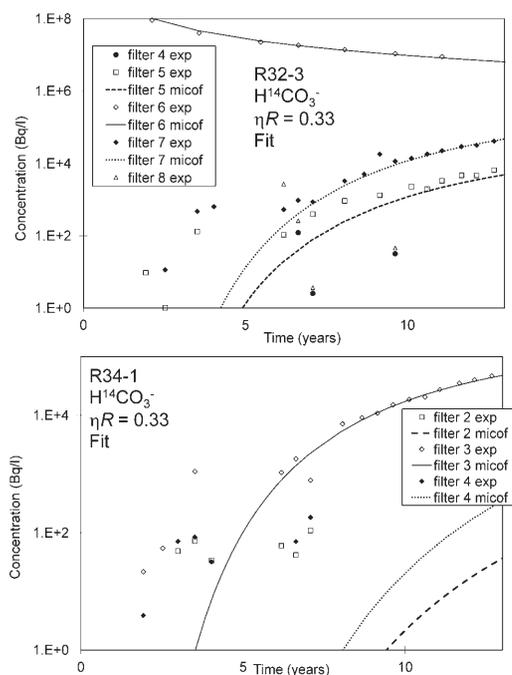
FIG. 13. Experimental data and fit in the filters of (the injection) piezometer R32-3 (top), and piezometer R34-1 (the piezometer parallel to the injection piezometer) of the Tribicarb-3D experiment (tracer: $H^{14}CO_3^-$). In the filters for which no MICOF prediction is shown, the prediction is lower than the lowest value in the figure.
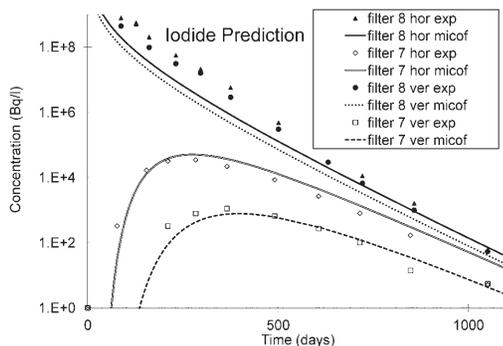
FIG. 14. Blind prediction of the iodide concentration in the TD41HV experiment (hor is the horizontal piezometer, ver is the vertical piezometer).

agreement between experimentally determined and predicted concentration is reasonable.

Although the agreement between experimental data and the prediction by the fit is not always good (Fig. 14), the optimal values agree well with the values used for the blind prediction: an apparent diffusion coefficient in the direction parallel to the bedding plane $D_{app,//} \approx 2.6 \times 10^{-10}$ m^2/s and an apparent diffusion coefficient in the direction perpendicular to the bedding plane $D_{app,\perp} \approx 1.4 \times 10^{-10}$ m^2/s. Due to the good agreement between the parameter values of the blind prediction and those fitted, we do not add a figure showing the experimental data next to the fit.

Natural Organic Matter migration in TD41HV

In order to understand the migration behaviour of Organic Matter in Boom Clay better, large-scale and long-term *in situ* migration experiments were initiated using the TD41HV piezometers. Transport of organic matter is complicated due to its colloidal nature which may result in filtering processes related to the Boom Clay porosity. Starting from laboratory-derived data interpreted by the classical diffusion retardation, extra complexity was introduced to account for the colloidal behaviour. This first attempt, which is not discussed further here, resulted in a reasonable fit of the experimental data (Martens *et al.*, 2010) but further fine tuning is needed.

CONCLUSIONS

With respect to the small-scale *in situ* migration experiments, only strontium and caesium can be

described by the classical diffusion retention formalism. Modelling the tracer profiles in the clay leads to apparent diffusion coefficients (7×10^{-12} m^2/s for strontium, 1×10^{-13} m^2/s for caesium) which are consistent with the values determined via laboratory experiments on clay cores sampled from the vicinity of the URF.

Large-scale (of the order of metres) *in situ* experiments were performed with non-retarded or slightly retarded tracers (HTO, iodide and H^{14}CO$_3^-$) and with ^{14}C labelled Natural Organic Matter. The tracer migration behaviour of HTO, iodide and H^{14}CO$_3^-$ was predicted at the start of the experiments based on migration parameters measured in laboratory experiments, and compared afterwards with the *in situ* experimental data. In general, the blind predictions provide excellent (CP1) to reasonable (Tribicarb-3D and TD41HV) agreement with the experimental data. Fitting the experimental *in situ* data leads to a diffusion coefficient parallel to the clay bedding plane of $\sim 4 \times 10^{-10}$ m^2/s and 5×10^{-10} m^2/s for HTO, 1×10^{-10} m^2/s for H^{14}CO$_3^-$ and 3×10^{-10} m^2/s for iodide and to a diffusion coefficient perpendicular to the bedding plane of 2×10^{-10} m^2/s for HTO, 1×10^{-10} m^2/s for H^{14}CO$_3^-$ and 1.5×10^{-10} m^2/s for iodide. These values are close the ones determined in lab experiments. All data were fitted with a simple analytical expression, and the HTO data were additionally fitted with COMSOL multiphysics, leading to about the same optimal values.

REFERENCES

Aertsens M., Put M. & Dierckx A. (1999) An analytical model for pulse injection experiments. Pp. 67−76 in: *Proceedings of 'Modelling of Transport Processes in Soils at Various Scales in Time and Space'*, Leuven, Belgium, 24-26 November 1999.

Aertsens M., Wemaere I. & Wouters L. (2004) Spatial variability of transport parameters in the Boom Clay. *Applied Clay Science*, **26**, 37−45.

Aertsens M., De Cannière P., Lemmens K., Maes N. & Moors H. (2008a) Overview and consistency of migration experiments in clay. *Physics and*

Chemistry of the Earth, **33**, 1019−1025.

Aertsens M., Van Gompel M., De Cannière P., Maes N. & Dierckx A. (2008b) Vertical distribution of $H^{14}CO_3^-$ transport parameters in Boom clay in the Mol-1 borehole (Mol, Belgium). *Physics and Chemistry of the Earth*, **33**, S61−S66.

Aertsens M., Maes N. & Van Gompel M. (2009a) Consistency of the strontium transport parameters in Boom Clay obtained from different types of migration experiments. Pp. 421−428 in: *Scientific Basis for Nuclear Waste Management XXIX* (B. Buratov & A. Aloy, editors.), *Materials Research Society Symposium Proceedings*, **1193**.

Aertsens M., De Cannière P., Moors H. & Van Gompel M. (2009b) Effect of ionic strength on the transport parameters of tritiated water, iodide and $H^{14}CO_3^-$ in Boom Clay. Pp. 497−504 in: *Scientific Basis for Nuclear Waste Management XXIX* (B. Buratov & A. Aloy, editors), *Materials Research Society Symposium Proceedings*, **1193**.

Altmann S., Tournassat C., Goutelard F., Parneix J.C., Gimmi T. & Maes N. (2012) Diffusion driven transport in clayrock formations. *Applied Geochemistry*, **27**, 463−478.

Bastiaens W., Bernier F. & Li X.L. (2007) SELFRAC: Experiments and conclusions on fracturing, self-healing and self-sealing processes in clays. *Physics and Chemistry of the Earth*, **32**, 600−615.

Baston G., De Cannière P., Ilett D., Cowper M., Pilkington N., Tweed C., Wang L. & Williams S. (2002) Technetium behavior in Boom Clay − a laboratory and field study. *Radiochimica Acta*, **90**, 735−740.

Bernier F. & Bastiaens W. (2004) Fracturation and self-healing processes in clays − The SELFRAC Project. Pp. 478−491 in: *Proceedings of EURADWASTE '04*, European Commission, Luxembourg, Report EUR21027.

Bourg I. (2004) *Diffusion of Water and Inorganic Ions in Saturated Compacted Bentonite.* Ph.D. Thesis, University of California, Berkeley.

Bruggeman C., Aertsens M., Maes N. & Salah S. (2010) *Iodine Retention and Migration Behavior in Boom Clay.* SCK − CEN, Mol, Belgium, report SCK − CEN-ER-119.

Crank J. (1975) *The Mathematics of Diffusion.* Clarendon Press, Oxford.

De Cannière P., Moors H., Lolivier P., De Preter P. & Put M. (1996) *Laboratory and in situ Migration Experiments in the Boom Clay*. European Commission, Luxembourg, Report EUR 16 927 EN.

Henrion P., Monsecour M., Fonteyne A., Put M., De Regge P. (1985) Migration of radionuclides in Boom Clay. *Radioactive Waste Management and the Nuclear Fuel Cycle*, **6** (3-4), 313−359.

Maes N., Salah S., Jacques D., Aertsens M., Van Gompel M., De Cannière P. & Velitchkova N. (2008) Retention of Cs in Boom Clay; Comparison of data from batch sorption tests and diffusion experiments on intact clay cores. *Physics and Chemistry of the Earth*, **33**, S149−S155.

Maes N., Bruggeman C., Govaerts J., Martens E., Salah S. & Van Gompel M. (2011) A consistent phenomenological model for natural organic matter linker migration of Tc(IV), Cm(II), NP(IV), Pu(III,IV) and Pa(V) in the Boom Clay. *Physics and Chemistry of the Earth*, **36**, 1590−1599.

Marivoet J. & Weetjens E. (2009) The importance of mobile fission products for long-term safety in the case of disposal of vitrified high-level waste and spent fuel in a clay formation. Pp. 31−42 in: *Mobile Fission and Activation Products in Nuclear Waste Disposal.* Workshop proceedings, La Baule, France, 16−19 January 2007, OECD/NEA, Issy-les-Moulineaux, France, OECD Nuclear Energy Agency, ISBN 978-92-64-99072-2.

Martens E., Maes N., Weetjens E., Van Gompel M. & Van Ravestyn L. (2010) Modelling of a large-scale in situ migration experiment with ^{14}C labeled natural organic matter in Boom Clay. *Radiochimica Acta*, **98**, 659−701.

Moors H. (2005) Topical report on the effect of the ionic strength on the diffusion accessible porosity of Boom Clay. SCK − CEN, Mol, Belgium, report SCK − CEN-ER-02.

Naves A., Samper J. & Gimmi T. (2012) Identifiability of diffusion and sorption parameters fom in situ diffusion experiments by using simultaneously tracer dilution and claystone data. *Journal of Contaminant Hydrology*, **142-143**, 63−74.

Noynaert L. (2000) Heat and radiation effects on the near filed of a HLW or spent fuel repository in a clay formation (CERBERUS project). EUR 19125 EN (Luxembourg, Office for Official Publications of the European Communities), ISBN 92-838-8913-0.

Put M., Monsecour M., Fonteyne A., Yoshida H. & De Regge P. (1989) In situ migration experiments in the Boom clay at Mol; experimental method and preliminary results. *Materials Research Society Symposium Proceedings*, **127**, 621−628.

Put M., De Cannière P., Moors H. & Fonteyne A. (1993) Validation of performance assessment model by large-scale in situ migration experiments. IAEA-SM-326/37, 319−326.

Samper S., Yi S. & Naves A. (2010) Analysis of the parameter identifiability of the in situ diffusion and retention (DR) experiments. *Physics and Chemistry of the Earth*, **35**, 207−216.

Weetjens E., Govaerts J. & Aertsens M. (2011) Model and parameter validation based on in situ experiments in Boom Clay. SCK − CEN, Mol, Belgium, report SCK − CEN-ER-171.

Weetjens E. & Maes N. (2013) Model validation based on in situ radionuclide migration tests in Boom Clay:

status of the CP1 experiment, 24 years after injection (submitted).

Wemaere I., Marivoet J. & Labat S. (2008) Hydraulic conductivity of the Boom Clay in north-east Belgium based on four core-drilled boreholes. *Physics and Chemistry of the Earth*, **33**, S24−S36.

Wersin P., Soler J., Van Loon L., Eikenberg J., Baeyens B., Grolimund D., Gimmi T. & Dewonck S. (2008) Diffusion of HTO, Br^-, I^-, Cs^+, $^{85}Sr^{2+}$ and $^{60}Co^{2+}$ in a clay formation: Results and modelling from an in situ experiment in Opalinus Clay. *Applied Geochemistry*, **23**, 678−691.

Yi S., Samper J., Naves A. & Soler J. (2012) Identifiability of diffusion and retention parameters of anionic tracers from the diffusion and retention (DR) experiment. *Journal of Hydrology*, **446−447**, 70−76.